

Fig. 3 Convergence of estimates for the pole locations for autoregressive filter (—) to actual pole values (---).

corresponding to the stable eigenvalue $\lambda = 0$ is X_k . The eigenvector corresponding to the marginally stable eigenvalue $\lambda = 1$ is in the $(n - 1)$ -dimension orthogonal subspace X_k^\perp . In general, $\lambda \in \{1 - L, 1\}$ with eigenvector $e \in \{X_k, X_k^\perp\}$, respectively. Therefore, $0 < L < 2$ guarantees marginal stability. Convergence of this parameter estimator is shown in Fig. 3.

Remark 4. For all L , the eigenvalue corresponding to X_k^\perp remains unity and only marginal stability of the observer can be realized. The entire parameter vector p can be estimated with asymptotically zero error if $X_k \neq 0$ and the direction of X_k varies. This variation is achieved by nonzero input excitation.

Remark 5. The standard parameter estimation projection algorithm, presented in Refs. 3 and 4, is a special case of the new observer presented here. By combining observer equations (30) and (31), the parameter estimation equation is

$$\rho_k = x_k - [F(X_{k-1})\hat{p}_{k-1} + u_{k-1}] \quad (34)$$

$$\hat{p}_k = A(X_{k-1})\hat{p}_{k-1} + L \frac{X_{k-1}}{X_{k-1}'X_{k-1}} \rho_k \quad (35)$$

The parameter identification algorithm from Ref. 3 is

$$\rho_k = x_k - F(X_{k-1})\hat{p}_{k-1} \quad (36)$$

$$\hat{p}_k = A_{k-1}\hat{p}_{k-1} + L \frac{X_{k-1}}{X_{k-1}'X_{k-1}} \rho_k \quad (37)$$

The new observer [Eqs. (34) and (35)] provides for an explicit forcing term and a state-dependent parameter dynamics matrix. (The observer in Ref. 3 can easily accommodate an input forcing function and probably can accommodate a state-dependent parameter dynamics matrix provided that the parameter variation bandwidth is much less than the bandwidth of the measured output.) The observer in Ref. 3 can be viewed as a special case of the new observer for which the full n -dimension state vector in Ref. 3, which is not directly measurable, becomes directly measurable by insertion of n unit delays into the measurement epoch.

VI. Conclusion

A new globally convergent nonlinear parameter estimator was developed. Unlike the conventional regression parameter estimators, this new observer estimates parameters of multistate systems for which all of the system states are simultaneously directly measurable. Because all states are directly, simultaneously measurable, a state-dependent parameter dynamics can be modeled in the new observer.

The first example demonstrated the new observer applied to a multistate system in which each state is simultaneously and directly measurable. The second example demonstrated that the conventional method of parameter estimation for a single-output autoregressive process is a special limited case of this new observer.

Synthesis of the new observer requires finding a satisfactory state-dependent gain matrix $M(x_k)$. Because no general form of $A(x_k)$ or $F(x_k, u_k)$ is assumed and even the dimension of $F(x_k, u_k)$ is not restricted, no general form of $M(x_k)$ is derived. The only stated requirement for selection of gain matrix $M(x_k)$ is that the eigenvalues

of $A(x_k) - M(x_k)F(x_k, u_k)$ be inside the unit circle. Experience has shown that, with insight into the system dynamics and a little imagination, a satisfactory $M(x_k)$ can usually be found.

References

- ¹Friedland, B., *Advanced Control System Design*, Prentice-Hall, Englewood Cliffs, NJ, 1995, pp. 318–324.
- ²Franklin, G. F., Powell, J. D., and Workman, M. L., *Digital Control of Dynamic Systems*, Addison-Wesley, Reading, MA, 1990, pp. 64–77.
- ³Åström, K. J., and Wittenmark, B., *Adaptive Control*, Addison-Wesley, Reading, MA, 1989, Chap. 3.
- ⁴Ljung, L., and Söderström, T., *Theory and Practice of Recursive Identification*, MIT Press, Cambridge, MA, 1986, Chap. 3.

Continuous Proximate Time-Optimal Control of an Aerodynamically Unstable Rocket

M. Kalyon*

Istanbul Technical University, 80626 Maslak,
Istanbul, Turkey

I. Introduction

TIME-OPTIMAL bang-bang control systems are often impractical because unavoidable measurement noise, disturbances, and nonideal components cause the bang-bang control to switch when the state does not exactly meet the switching criteria. This may degrade tracking performance and produce other bad effects such as a limit cycle about the target state. To reduce or eliminate such undesirable behavior, a number of nonlinear controllers that give near time-optimal response have been developed in the literature.^{1–4} McDonald³ introduced a method called a dual-mode concept, namely, linear mode and nonlinear mode. The dual-mode operation requires the generation of two arbitrary nonlinear functions. One generates the switching curve, and the other determines the boundary of the neighborhood used by the mode selector.

Recently, Workman⁵ proposed a controller called proximate time-optimal servomechanism (PTOS) for double-integrator plants. Reference 5 showed that the controller generates solutions that approach the exact minimum-time solutions when the system disturbances and the modeling errors vanish; hence, the term proximate or very near. The controller approximates the switching curve with a strip such that the optimal switching curve is centered along the strip. Unlike the bang-bang controller, the PTOS controller is continuous in the neighborhood of the strip. Near the origin, the PTOS controller switches to a linear feedback law; in this sense, the PTOS controller has dual-mode behavior.

Our approach is motivated by the work of Rauch and Howe.⁴ They introduced a controller for second-order systems that attempts to combine the best features of the dual-mode concept³ with ideas discussed in Ref. 2. The result is a proximate controller, which, unlike the PTOS controller, is a continuous nonlinear function of system state. We have generalized and developed the controller introduced by Rauch and Howe.⁴ We, thus, obtain continuous proximate time-optimal (CPTO) controllers, which give near time-optimal response for second-, third-, and higher-order systems.⁶ In this Note we present the CPTO controller designed for a second-order unstable plant. The CPTO controller provides nonlinear operation of the servo within a narrow strip in the neighborhood of the switching curve and near linear operation in a neighborhood of the origin,

Received Jan. 27, 1997; revision received April 24, 1997; accepted for publication April 29, 1997. Copyright © 1997 by the American Institute of Aeronautics and Astronautics, Inc. All rights reserved.

*Professor, Department of Aeronautics/Astronautics Engineering.

except for the small and rapidly diminishing effects of the nonlinear terms. The strip is constructed so that the switching curve is not centered within the strip, but rather the switching curve forms one of the boundaries of the strip. Near the origin, the strip is shifted so that it contains the origin in its center. The responses obtained by using the CPTO controller are near time optimal. Most importantly, the CPTO controller is proved to be asymptotically stable as long as the initial state is within the recoverable zone of the unstable plant.

II. Formulation of an Aerodynamically Unstable Rocket

We consider the pitch attitude control of a rocket that is thrusting in the atmosphere. If the center of aerodynamic pressure is ahead of the c.g. of the rocket, which is normally the case when the rocket is not provided with tail fins, then any slight angle of attack α caused by an aerodynamic disturbance produces a lifting force L perpendicular to the longitudinal axis of the rocket, which in turn causes a destabilizing moment.⁷ This is shown in Fig. 1, where q_α is the dynamic pressure. Control is achieved by changing the direction of the rocket thrust F through the angle δ . If we assume that the velocity is constant, δ is small, and also that L is proportional to α , that is, $L = c_1 q_\alpha \alpha$, then we obtain the following pitching moment equation about the c.g.⁷:

$$I\ddot{\alpha} - c_1 q_\alpha c \alpha + F \delta d = 0 \quad (1)$$

where d is the distance as shown in Fig. 1, F is the thrust magnitude, and I is the pitch axis inertia. Letting $k = c_1 q_\alpha c$ and $u = F \delta d$, we obtain

$$I\ddot{\alpha} - k\alpha = -u \quad (2)$$

which is an unstable plant with transfer function $1/(k - Is^2)$, where $I, k > 0$. Furthermore, if the maximum thrust-vector-control angle is given by δ_{\max} , then $|u| \leq u_m$, where $u_m = F \delta_{\max} d$, so that we have effort-limited control. Defining the state variables $x_1 = \alpha(t)$ and $x_2 = \dot{\alpha}(t)$, and assuming zero reference command signal $[r(t) = 0]$, the equations describing the system (2) then become

$$\dot{x}_1 = x_2, \quad \dot{x}_2 = \omega_n^2(x_1 - u/k) \quad (3)$$

where $\omega_n = \sqrt{k/I}$ is the undamped natural frequency. We can rewrite Eq. (3) in vector differential equation form as

$$\dot{x} = Ax + Bu, \quad A = \begin{bmatrix} 0 & 1 \\ \omega_n^2 & 0 \end{bmatrix}, \quad B = \begin{bmatrix} 0 \\ -\omega_n^2/k \end{bmatrix} \quad (4)$$

Without loss of generality, we assume that $u_m = 1$, that is, $u(t) \leq 1$ for all t .

Our objective is to determine the control that forces any given initial state $x(0)$ within the recoverable zone (RZ) of the unstable plant to the origin in minimum time. Before we proceed, we need to define the RZ of the unstable plant as follows^{7,8}:

$$\text{RZ} = \{x(0): \text{there exist } \bar{t} > 0 \text{ and } u(t) \text{ such that } |u(t)| \leq 1 \text{ and } x(\bar{t}) = 0\}$$

If $x(0) \notin \text{RZ}$, there does not exist any admissible control that drives the state to the origin. Therefore, before designing a time-optimal controller for the unstable plant (4), one should obtain its RZ.

III. Computation of the RZ

The eigenvalues of the system (4) are $\pm \omega_n$. Because the eigenvalues are distinct, we may use a similarity transformation, $x = Py$, to reduce the matrix A in Eq. (4) to its diagonal form, where

$$x = [x_1 \ x_2]^T, \quad y = [y_1 \ y_2]^T, \quad \text{and} \quad P = \begin{bmatrix} 1 & -1 \\ \omega_n & \omega_n \end{bmatrix}$$

Thus, we obtain

$$\dot{y}_1 = \omega_n \frac{y_1 - 0.5u}{k}, \quad \dot{y}_2 = -\omega_n \frac{y_2 + 0.5u}{k} \quad (5)$$

Clearly, $y_2(t)$ is a stable state variable; however, for $|y_1| \geq 0.5/k$, y_1 cannot be driven to the origin. Obviously, RZ must be a subset of the remaining region where $|y_1| < 0.5/k$. It can be shown from time-optimal control theory that the solution of Eq. (5), originating within the set where $|y_1| < 0.5/k$, reaches the ideal switching curve of Eq. (5), and then it moves on the switching curve until it reaches the origin. Thus, the RZ of Eq. (5) is

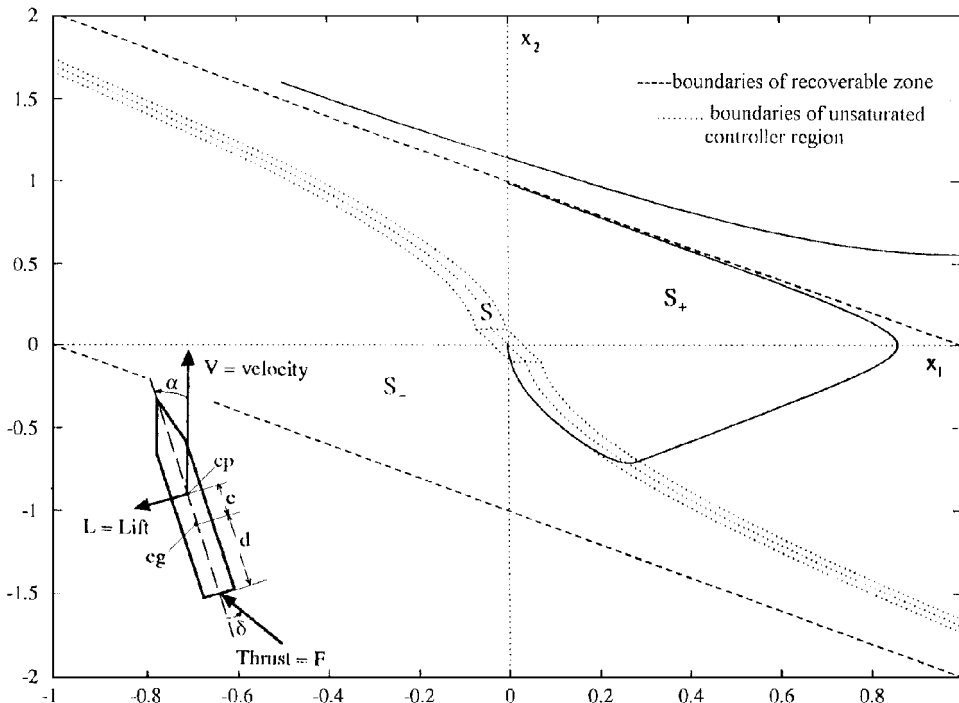


Fig. 1 Aerodynamically unstable rocket³ and the solution paths of the system: $\omega_n = 1$, $k = 1$, $k_1 = 30$, and $k_2 = \frac{1}{3}$.

$RZ_y = \{y: |y_1| < 0.5/k\}$. The corresponding RZ for Eq. (4), obtained by using $y = P^{-1}x$, becomes

$$RZ = \left\{ x: \left| \frac{x_1 + x_2}{\omega_n} \right| < \frac{1}{k} \right\}$$

IV. Ideal Time-Optimal Controller for the Plant

Because the time-optimal control exists and is unique for all $x(0) \in RZ$ (Ref. 9), we can apply the necessary conditions to characterize the time-optimal control.¹⁰ It must be one of the sequence $\{+1\}, \{-1\}, \{+1, -1\}, \{-1, +1\}$, and we can use backward integration to characterize the optimal trajectories leading to the origin.⁶ Let τ represent negative time, as opposed to positive time t , and rewrite Eq. (3); for backward time τ , we have

$$\frac{dx_1}{d\tau} = -x_2, \quad \frac{dx_2}{d\tau} = -\omega_n^2 \left[x_1 - \frac{u}{k} \right] \quad (6)$$

where $x(0) = 0$ and $\tau > 0$. For $u(\tau) = \Delta^* = \pm 1$, this gives

$$x_1(\tau) = -\frac{0.5\Delta^*}{k}(e^{\omega_n\tau} + e^{-\omega_n\tau} - 2) \quad (7)$$

$$x_2(\tau) = \frac{0.5\omega_n\Delta^*}{k}(e^{\omega_n\tau} - e^{-\omega_n\tau})$$

We solve for τ from the $x_2(\tau)$ equation of Eqs. (7), use the fact that τ must be positive, and organize the resulting equations, and we obtain,⁶ after some lengthy algebra,

$$\Delta^* = \text{sgn}(x_2) \quad (8)$$

Substituting the resulting $\tau(x_2)$ into the $x_1(\tau)$ equation of Eqs. (7), we obtain the following characterization of the switching curve:

$$x_1 = X_1(x_2) = (\Delta^*/k) \left[1 - \sqrt{1 + (kx_2/\omega_n)^2} \right] \quad (9)$$

$$\Delta^* = \text{sgn}(x_2)$$

Thus, the discontinuous, time-optimal, bang-bang control law is $U^*(x)$, where

$$U^*(x) = \begin{cases} \text{sgn}[x_1 - X_1(x_2)] & \text{if } x_1 - X_1(x_2) \neq 0 \\ \text{sgn}[x_2] & \text{if } x_1 - X_1(x_2) = 0 \end{cases} \quad (10)$$

V. CPTO Controller for the Plant

The form of the CPTO control law (which is motivated by Rauch and Howe⁴) is obtained as follows. First, we try an obvious modification of the bang-bang controller. A continuous controller, $U'(x) \approx U^*(x)$, is defined as follows:

$$U'(x) = \text{sat}\{k_1[x_1 - X_1(x_2)]\}, \quad k_1 = 1/e_1 \quad (11)$$

where

$$\text{sat}(x) = \{+1 \text{ for } x \geq +1, \quad x \text{ for } |x| < 1, \quad -1 \text{ for } x \leq -1\}$$

We note from Eqs. (9) and (11) that, when $x_2 \cong 0$ and $x < e_1$, then $U'(x)$ becomes $U'(x) \cong x_1/e_1$. Substituting $u = U'(x) = x_1/e_1$ into the state equations (3), we obtain

$$\ddot{x}_1 - \omega_n^2 b x_1 = 0, \quad b = 1 - 1/ke_1$$

Clearly, for any value of b , the continuous controller U' causes problems near $x = 0$. We want, ideally, $U(x) \cong U^*(x)$ for $\|x\|$ large and $U(x) \cong k_1(x_1 + k_2x_2)$ for $\|x\|$ small, where k_1 and k_2 can be specified arbitrarily. This goal can be achieved by replacing x_1 by $x_1 - X_1(x_2)$ [noting that $X_1(x_2)$ is second order in x_2 and has a negligible effect near origin] and limiting the term k_2x_2 so that it has little effect for $|x_2|$ sufficiently large. Finally, the whole expression needs to be limited as in U' . This suggests

$$U(x) = \text{sat}\{k_1[x_1 - X_1(x_2) + e_2 \text{sat}(k_2x_2/e_2)]\} \quad (12)$$

For $x_2 > e_2/k_2$, Eq. (12) gives

$$U(x) = \text{sat}\{k_1[x_1 - X_1(x_2) + e_2]\} \quad (13)$$

What is a good choice for e_2 ? This can be best seen by examining Eq. (13) when $U(x) = +1$. In this case, $k_1[x_1 - X_1(x_2) + e_2] \geq 1$, which implies $x_1 - X_1(x_2) \geq -e_2 + 1/k_1$.

Thus, we let $1/k_1 = e_2$ to obtain the original switching curve for the place where saturation at $+1$ occurs. Notice that, for $x_2 < -e_2/k_2$, the same thing happens for the place where saturation at -1 occurs. Thus, the continuous feedback

$$U(x) = \text{sat}\{k_1[x_1 - X_1(x_2) + e_1 \text{sat}(k_1k_2x_2)]\}, \quad e_1 = 1/k_1 \quad (14)$$

achieves the desired result of $U(x) = U^*(x)$ for $x \in \{x: x_1 - X_1(x_2) = 0\}$ and $|x_2| > e_2/k_2$. Notice that, for $|x_2| > e_2/k_2$, the width of the unsaturated region along the x_1 axis is $2/k_1$. Thus, making the linear gain k_1 large improves the approximation $U(x) \cong U^*(x)$. Again, we remark that, when $\|x\|$ is small, from Eqs. (9) and (14) we have

$$U(x) \cong k_1(x_1 + k_2x_2) \quad (15)$$

The solutions shown in Fig. 1 for the CPTO controller are almost indistinguishable from those of an ideal time-optimal bang-bang controller. We observe from Fig. 1 that, if a trajectory originates within the recoverable set, it reaches the unsaturated controller region, where the control changes polarity and drives the trajectory to the origin. We also observe from Fig. 1 that, if a trajectory originates outside the recoverable set, the motion of the closed-loop system diverges. Note that a linear saturating controller $U'(x) = \text{sat}\{k_1(x_1 + k_2x_2)\}$ performs very poorly by comparison.

VI. Stability of the CPTO Control System

We know from linear control theory that the system (4) with the controller $u = k_1(x_1 + k_2x_2)$ is stable if $k_1 > k$ and $k_2 > 0$. Thus, these conditions must also hold for the system (4) with the CPTO controller (14).

Theorem: Let $\beta_1 = k_1k_2\omega_n^2$, $\beta_2 = \sqrt{(1 + \omega_n^2k^2)}$. For all $x(0) \in RZ$, the solution of Eq. (3) with controller (14) is asymptotically stable, $t > 0$ and $x(t) \rightarrow 0$ as $t \rightarrow \infty$, if

$$\begin{aligned} k_1 &> k, & k_2 &> 0, & \beta_1 &> 1 \\ k &< k_1(2 - \beta_2), & k_1 &> k(1 + 0.5\beta_1\beta_2) \end{aligned} \quad (16)$$

Before we begin the proof, we introduce the following notation:

$$\begin{aligned} S_- &= \{x \in RZ : \mu(x) \leq -1\}, & S &= \{x \in RZ : |\mu(x)| < 1\} \\ S_+ &= \{x \in RZ : \mu(x) \geq 1\} \end{aligned} \quad (17)$$

where

$$\mu(x) = k_1[x_1 - X_1(x_2) + e_1 \text{sat}(k_1k_2x_2)], \quad e_1 = 1/k_1 \quad (18)$$

We remark that $S_- \cup S \cup S_+ = RZ$. The regions S_+ , S_- , and S are shown in Fig. 1.

Proof: The proof consists of three parts, which are motivated in some aspects by Refs. 5 and 12.

1) All trajectories originating within RZ but outside of S enter S in a finite time.⁶

2) All trajectories originating within S remain within S . We know that S is the region within which the first saturation function in the u equation (14) is unsaturated. That is, $u = U(x) = \mu(x)$. Thus, the region S is bounded from above by the boundary on which $u = +1$ and bounded from below by the boundary on which $u = -1$ (as shown in Fig. 1). To prove that any trajectory originating within S remains within S , it is sufficient to show that, when $x \in S$ is near the boundary of S , where $U(x) \cong +1$, then $\dot{\mu}(x) \leq 0$, and when $x \in S$ is near the boundary of S where $U(x) \cong -1$, then $\dot{\mu}(x) \geq 0$. Equivalently, $\dot{\mu}(x) \leq 0$, where $\mu(x) = 1$, and $\dot{\mu}(x) \geq 0$, where $\mu(x) = -1$. Use of Eq. (16), after some lengthy algebra,⁶ proves part 2.

3) There exists a Lyapunov function when $x \in S$.
Consider

$$V = \omega_n^2[(k_1/k) - 1]x_1^2 + x_2^2, \quad k_1 > k \quad (19)$$

then $x \in S$ implies

$$U(x) = k_1(x_1 - X_1) + \text{sat}(k_1 k_2 x_2) \quad (20)$$

Computing \dot{V} from Eq. (19) and substituting Eqs. (3) and (20) into the \dot{V} equation yields

$$\begin{aligned} \dot{V} &= -2k_1(\omega_n^2/k^2)x_2 \text{sgn}(x_2)(\Lambda - 1) - 2(\omega_n^2/k)x_2 \text{sat}(k_1 k_2 x_2) \\ \Lambda &= \sqrt{1 + (kk_2/\omega_n)^2} \quad (21) \end{aligned}$$

Because $\Lambda \geq 1$, it follows from Eq. (21) that $\dot{V} \leq 0$ and $\dot{V} = 0$ if and only if $x_2 = 0$. Because $\dot{V} = 0$ for $x_2 = 0$, we must show that $x = 0$ is the only invariant subset of $\{x: x_2 = 0\}$. Substituting $x_2 = 0$ into Eqs. (9) and (14), we obtain $U = u = k_1 x_1$. Thus, for $x_1 \neq 0$, then $U = u \neq 0$, which implies from Eq. (3) that $\dot{x}_2 = -\omega_n^2[(k_1/k) - 1]x_1 \neq 0$ and x_2 becomes nonzero. Hence, $x = 0$ is the only invariant set, and La Salle's theorem¹¹ completes the proof.

VII. Conclusions

We have presented a nonlinear feedback law for an aerodynamically unstable rocket. This is proximate time-optimal in the sense it marches near minimal-time behavior. Unlike the proximate time-optimal laws of Pao and Franklin,¹² it is continuous and, thus, produces a continuous control function that is likely to produce little response in the presence of small plant imperfections. For states near the origin, the nonlinear law approximates the linear law $k_1(x_1 + k_2 x_2)$, where k_1 and k_2 can be chosen from a satisfactorily large set of values. Finally, it has been shown that the system is asymptotically stable as long as the initial state is within the RZ of the unstable plant.

CPTO laws for two more second-order plants, including the double-integrator plant, have been obtained.⁶ CPTO laws for third- and higher-order systems have also been obtained.⁶

Acknowledgments

The author wishes to acknowledge R. M. Howe and E. G. Gilbert for their constructive comments, many valuable discussions, and the insight they offered.

References

- Kalman, R. E., "Analysis and Design Principles of Second and Higher Order Saturating Servomechanisms," *Transactions of the American Institute of Electrical Engineering*, Vol. 74, Sept. 1955, pp. 102–118.
- Lewis, J. B., "The Use of Nonlinear Feedback to Improve the Transient Response of a Servomechanism," *Transactions of the American Institute of Electrical Engineering*, Pt. 2, Vol. 71, 1953, pp. 449–453.
- McDonald, D. C., "Multiple Mode Operation of Servomechanisms," *Review of Scientific Instruments*, Vol. 23, Jan. 1952, pp. 22–30.
- Rauch, L. L., and Howe, R. M., "A Servo with Linear Operation in a Region About the Optimum Discontinuous Switching Curve," *Proceedings of the Symposium on Nonlinear Circuit Analysis*, Polytechnic Inst. of Brooklyn, Brooklyn, NY, 1956, pp. 215–223.
- Workman, M. L., "Adaptive Proximate Time-Optimal Control: Continuous Time Case," *Proceedings of the 1987 American Control Conference* (Minneapolis, MN), 1987, pp. 589–594.
- Kalyon, M., "Continuous Proximate Time-Optimal Control of Servomechanisms," Ph.D. Thesis, Aerospace Engineering Dept., Univ. of Michigan, Ann Arbor, MI, May 1993.
- Howe, R. M., "Nonlinear Control Systems," Aerospace Engineering Dept., Univ. of Michigan, Ann Arbor, MI, 1982.
- LeMay, J. L., "Recoverable and Reachable Zones for Control Systems with Linear Plants and Bounded Controller Outputs," *IEEE Transactions on Automatic Control*, Vol. AC-9, Oct. 1964, pp. 346–354.
- Lee, E. B., and Markus, L., *Foundation of Optimal Control Theory*, Wiley, New York, 1967, pp. 259–273.
- Athans, M., and Falb, P. L., *Optimal Control: An Introduction to the Theory and Its Applications*, McGraw-Hill, New York, 1966, pp. 395–410.
- La Salle, J., and Lefschetz, S., *Stability by Lyapunov's Direct Method: With Applications*, Academic, New York, 1961, p. 58.

¹²Pao, L. Y., and Franklin, G. F., "Proximate Time-Optimal Control of Third-Order Servomechanisms," *IEEE Transactions on Automatic Control*, Vol. 38, 1993, pp. 560–580.

Evaluation of Practical Solutions for Onboard Aircraft Four-Dimensional Guidance

Patrick Hagelauer* and Félix Mora-Camino†
Laboratoire d'Analyse et d'Architecture des Systèmes,
31077 Toulouse, France

Introduction

ONE of the principal goals of flight management systems (FMS) is to optimize the flight parameters to minimize fuel- and time-related costs. With the sustained increase of commercial air traffic during the last decades, capacity and congestion problems have become relevant for airspace and terminal traffic controllers, and time constraints have been imposed on particular flights. Such time constraints can be found at a terminal airspace, where it can be necessary to arrive at specified time to be allowed direct access to the runway.

In earlier versions of FMS, no time constraints were explicitly taken into account and the time of crossing at any waypoint was the result of the aircraft trajectory optimization process, minimizing a global criterion mixing fuel- and time-related costs and, therefore, did not necessarily match any desired arrival time constraint.

Recently, new functionalities have been made available on some modern aircraft to allow the control of crossing time at any waypoint of the flight plan. Practical solutions typically seek to adjust the so-called cost index, which is a parameter used by the airlines to combine fuel and time costs to obtain a new speed profile that is consistent with the time constraint while the altitude cruise profile is either frozen or adjusted in a limited way.¹ This solution approach has been considered by some authors as near optimal with respect to fuel costs.^{1,2}

In this Note, the optimal control theory is used to show that this is not necessarily the case. The cost-index-based solution is compared, on theoretical and quantitative bases, to the optimality conditions resulting from the formulation of a cruise optimization problem with an explicit crossing time constraint.

Practical Solutions for Time-Constrained Flight

This study is restricted to the cruise phase, which represents the main part of a long-range flight. During cruise, the main constraints are to fly at selected legal air traffic control levels and to match an imposed time constraint T_c at some given crossing point.

The objective of the cruise flight optimization consists here in determining the best cruise flight altitudes and speed profile to satisfy the given time constraint while minimizing total fuel burn.

Fixed-Cost-Index-Based Solutions

A typical class of solutions for this problem is that of the cost-index-based approaches. In this case, the cruise phase is discretized into a succession of constant altitude and constant Mach number segments. The solution is generated by computing online, over each segment, the optimum cruise speed that minimizes the mean flight cost over the given flight segment. Here total flight cost is defined as

$$\text{cost} = \text{fuel} + \text{CI} \times \text{time} \quad (1)$$

Received Oct. 11, 1996; revision received May 2, 1997; accepted for publication May 12, 1997. Copyright © 1997 by the American Institute of Aeronautics and Astronautics, Inc. All rights reserved.

*Research and Development Engineer, Aérospatiale, 7, Avenue du Colonel Roche.

†Professor, Ecole Nationale de l'Aviation Civile, 7, Avenue du Colonel Roche.